JGP Journal of General Physiology

VIEWPOINT

Investigation into the mechanism of thin filament regulation by transient kinetics and equilibrium binding: Is there a conflict?

David H. Heeley[1], Howard D. White[2], and Edwin W. Taylor[3]

Striated muscle contraction occurs when myosin undergoes a lever-type structural change. This process (the power stroke) requires ATP and is governed by the thin filament, a complex of actin, tropomyosin, and troponin. The authors have used a fast-mixing instrument to investigate the mechanism of regulation. Such (pre–steady-state kinetic) experiments allow biochemical intermediates in a working actomyosin cycle to be monitored. The regulatory focal point is demonstrated to be the step that involves the departure of inorganic phosphate (i.e., AM-ADP-Pi → AM-ADP). This part of the cycle, which lies on the main kinetic pathway and coincides with the drive stroke, is maximally accelerated ∼100-fold by the combined association of ligands (Ca[II] and rigor myosin heads) with the thin filament. However, the observed ligand dependencies of the rates of Pi dissociation that are reported herein are at variance with predictions of models derived from experiments where ATP hydrolysis is not taking place (and myosin exists in a nonphysiological form). It is concluded that the principal influence of the thin filament is in setting the rate of Pi dissociation and that physiological levels of regulation are dependent upon the liganded state of the thin filament as well as the conformation of myosin.

Introduction

The striated muscle thin filament is a repeating assembly of the proteins actin, tropomyosin, and troponins I, C, and T. An extensive network of connections exist between the various components. When ligands (either Ca[II] or rigor myosin-S1) associate with the thin filament, there is a perturbation in the network that ultimately leads to contraction. When they dissociate, the muscle relaxes.

Understanding of the details of the regulatory mechanism has changed over the years. Steric interference of myosin binding by tropomyosin-troponin (Haselgrove, 1972; Huxley, 1972; Parry and Squire, 1973) offered an attractive molecular explanation for how regulation occurred but was subsequently found to be a minor part of the mechanism (Chalovich and Eisenberg, 1982). The models of Hill envisaged two structural thin filament states (Hill et al., 1980, 1983). The most widely cited model envisages three such states (blocked, closed, and open; McKillop and Geeves, 1993; Lehman, 2017). These models were derived from equilibrium binding and other experiments in which myosin (M) is not hydrolyzing ATP. Our approach has been to first identify the regulated step in an active actomyosin cycle with a view to then comparing the thin filament ligand sensitivity of different myosin conformers.

Stopped-flow kinetics are ideally suited to investigating the issue of regulation of actomyosin ATP hydrolysis and muscle contraction. In multi-mixing mode, myosin subfragments and ATP are first mixed for 1–2 s to produce the steady-state intermediates (i.e., M-ATP and M–ADP–inorganic phosphate [Pi]) followed by mixing with thin filaments at various stages of activation by ligand (Fig. 1). Such experiments are typically performed at high concentrations of actin and well below physiological ionic strength, due to the highly salt-sensitive interaction of myosin and actin. The availability of reporter probes has enabled specific steps in the cycle (i.e., Pi and ADP dissociation) to be measured. In this work, fluorescent nucleotides and a Pi binding protein have been used. Such reagents are designed only to respond to changes in chemical states. With either type of probe, Pi dissociation (AM-ADP-Pi → AM-ADP + Pi) is demonstrated to be the dominant regulatory mechanism (Heeley et al., 2002, 2006; Houmeida et al., 2010). The combined binding of Ca(II) and rigor myosin-S1 to the thin filament produces a substantial (80–140-fold) activation in the rate of the Pi

[1]Department of Biochemistry, Memorial University, St. John's, Canada; [2]Department of Physiological Sciences, Eastern Virginia Medical School, Norfolk, VA; [3]Department of Molecular Genetics and Cell Biology, University of Chicago, Chicago, IL.

Correspondence to David Heeley: dheeley@mun.ca

This work is part of a special collection on myofilament function.

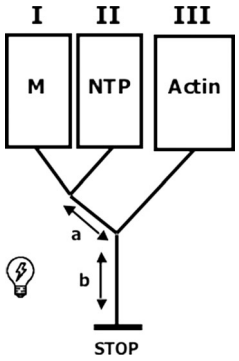

Figure 1. **Schematic of double-mixing stopped flow method.** Double-mixing stopped-flow apparatus. First mix: myosin-S1 (M) in syringe I is mixed with NTP (either ATP or md-ATP) in syringe II and allowed to incubate for 1–2 s in the delay line (a) to attain steady-state binding and hydrolysis of the substrate by myosin alone. The time of the delay was determined from knowledge of rate constants of nucleotide binding and steady-state hydrolysis determined from the rate of formation and composition of intermediates in the delay line as analyzed by quench flow (White et al., 1997). Second mix: the steady-state intermediates are combined with actin (A) or thin filaments (actin plus tropomyosin and troponin) contained in syringe III. After the second mix, the solution enters the flow cell (b), where the rate of phosphate dissociation is measured either from phosphate binding to (N-[2-(1-maleimidyl)ethyl]-7-(diethylamino)coumarin-3-carboxamide (MCDD) phosphate binding protein (excitation, 430 nm; emission >450 nm) or the observed rate of md-ADP dissociation from actomyosin-md-ADP-Pi (excitation, 360 nm; emission >420 nm). Product dissociation from myosin and actomyosin is an ordered mechanism in which phosphate dissociates first and therefore limits the rate of nucleoside diphosphate dissociation. Thus the fluorescence change associated with md-ADP dissociation can be used to measure phosphate dissociation.

dissociation step. In contrast, the dissociation of nucleoside diphosphate from post–power stoke myosin is only accelerated 10–12-fold. Thus, regulation is dependent on the thin filament state and also the conformation of the myosin head (pre– vs. post–power stroke).

Early studies of product release

A number of techniques have been used to investigate the kinetic properties of the myosin (or actomyosin)–product complex, including proton release (Finlayson and Taylor, 1969), changes in intrinsic fluorescence (Bagshaw and Trentham, 1973), and oxygen exchange (Pi/water; Bagshaw and Trentham, 1973). The first "definitive" measurement involved rapid size-exclusion chromatography (Taylor et al., 1970; Lymn and Taylor, 1971). Performed at low temperature to reduce the rate of reaction, the rate of chemical hydrolysis on myosin alone was demonstrated to be some 100-fold faster than the maximum steady-state MgATPase (hydrolysis) rate, indicating that product dissociation (from myosin) is rate-limiting and stimulated by actin. These and other observations led to the formulation of the Lymn–Taylor model (Lymn and Taylor, 1971). Quoting from their 1971 paper, "The essential features are that actomyosin dissociation precedes hydrolysis and activation is produced by recombination of actin with the myosin products complex with displacement of product." The model provided a biochemical explanation for contraction and is still relevant today.

How do tropomyosin and troponin regulate the actomyosin cycle?

The Steric Blocking hypothesis proposed that tropomyosin physically hinders the complexation of actin and myosin at low [Ca(II)] but not high (Haselgrove, 1972; Huxley, 1972; Parry and Squire, 1973). However, measurement of the affinity of myosin-S1-ATP and S1-ADP-Pi for thin filaments by time-resolved light scattering (Chalovich et al., 1981) and sedimentation (Chalovich and Eisenberg, 1982) showed the effect of Ca(II) on binding was disproportionately small (approximately twofold) when compared with the effect on the ATPase rate. From these results, it became apparent that regulation could not operate on the basis of a simple steric blocking mechanism. Quoting from Chalovich and Eisenberg (1982), "These data do not support a simple steric blocking model of muscle relaxation. Rather they suggest that, in the absence of Ca(II), troponin-tropomyosin inhibits a kinetic step, perhaps Pi release, in the cycle of ATP hydrolysis."

The above proposal was investigated (Rosenfeld and Taylor, 1987a) using a double-mixing stopped-flow spectrofluorimeter in conjunction with the fluorescent nucleotide etheno-ATP, a base-modified analogue (Secrist et al., 1972). The custom-made instrument was pressure-driven with a dead-time of 1–2 ms. An intermix adjustable delay allowed for the selection of a steady-state mixture of myosin bound with either substrate (M-NTP) or products (M-NDP-Pi). The mixture was combined, in the second mix, with thin filaments (either at pCa 4 or 8) containing ATP to eliminate any unwanted rigor activation, and "decay" of the pre–power stroke complex was then monitored for a single turnover of the cycle. The observed rates of the fluorescence changes when plotted against concentration conformed to hyperbolae that extrapolated to maxima of 20–25 (pCa 4) and 1 (pCa 8) per second, at least a 20-fold induction. At the same time, the bound hydrolysis rate was comparatively insensitive to Ca(II) (less than twofold as determined by quench flow). This study provided the first real insight into the mechanism of Ca(II) regulation.

A significant advance in the field was the development of an inorganic phosphate reporter protein (Brune et al., 1994). Bacterial Pi binding protein (PBP) is synthesized in response to Pi starvation whereupon it accumulates in the periplasmic space. It is small, monomeric, contains a single, high-affinity site (K_d, 100 nM), and binds Pi rapidly (rate constant, k, 1.4×10^8 M^{-1} s^{-1}). Furthermore, the 3-D structure had been solved (Luecke and Quiocho, 1990). Covalent linkage of a coumarin derivative to cysteine-197 (introduced adjacent to the binding cleft) created a reagent having Pi-sensitive emission (Brune et al., 1994). Armed with the fluorescently labeled PBP, it became feasible to track Pi transients directly. Examples are presented in Fig. 2, A and B.

Effect of unregulated actin on Pi release

Essentially the same single-turnover, double-mixing approach of Rosenfeld and Taylor (1987a) was taken by White and coworkers in which they were able to use the natural substrate ATP. Using fluorescent PBP, a 1,000-fold acceleration of the rate of dissociation of Pi from pre–power stroke myosin-S1-ADP-Pi by actin relative to myosin alone was demonstrated (White et al., 1997). In these experiments, actin binds to myosin-ATP and

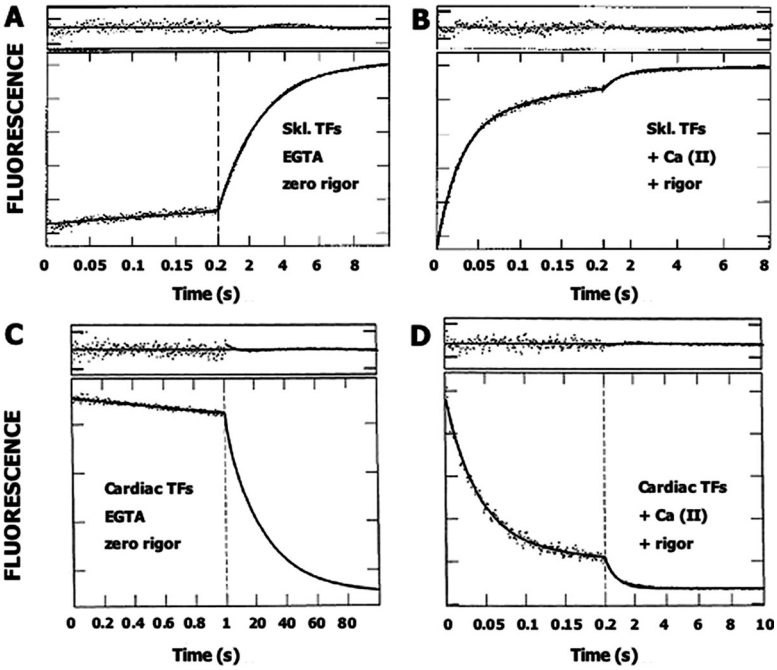

Figure 2. **Examples of time course of phosphate release from regulated acto-myosin-NDP-Pi as monitored with phosphate binding protein or md-ATP.** Time course of fluorescence change (A–D). The residuals at the top of each trace show the difference between the fit curve and the data. **(A and B)** Double mixing experiments were performed with fluorescent PBP and skeletal muscle proteins. Data taken from Heeley et al. (2002). All solutions contained ~10-fold excess of PBP versus ATP to ensure binding of any liberated Pi, as well as a Pi scavenging system (Brune et al., 1994). The intervening period (delay time) between the first and second mixes was carefully selected so as to have the maximal amount of M-ADP-Pi and minimal M-ADP before the second mix. The effect of rigor S1 binding was investigated by having a surplus of myosin-S1A1 versus ATP in the first mix so that excess was available to bind to the thin filaments, before Pi dissociation, in the second mix. Ionic strength, ~12 mM. A fuller description of the conditions is to be found in Heeley et al. (2002). **(A)** Phosphate dissociation from "turned-off" (no bound ligands) regulated AM-ADP-Pi. First mix, 2 µM myosin-S1A1 + 2 µM ATP. Delay, 1 s. Second mix, reconstituted skeletal thin filaments containing EGTA. Final concentrations in the flow cell were 0.44 µM myosin-S1, 0.44 µM nucleotide, 28 µM regulated actin (0.3 mM EGTA), 2.7 mM $MgCl_2$, 5 µM PBP, and 5 mM MOPS buffer, pH 7, 20°C. The thin filament concentration is expressed here and throughout in terms of the actin subunit concentration. The solid line is an average of three shots and the best fit to a single exponential equation I(t) = 1.0 exp −0.4t + C. **(B)** Phosphate dissociation from "turned-on" (bound Ca[II] and bound rigor myosin-S1) regulated AM-ADP-Pi. First mix, 20 µM myosin-S1A1 + 2 µM ATP, incubated for 1 s and then mixed with reconstituted thin filament. Final concentrations in the flow cell were 3.96 µM free myosin-S1, 0.44 µM nucleotide, 28 µM regulated actin (0.3 mM $CaCl_2$), 2.7 mM $MgCl_2$, 5 µM PBP, and 5 mM MOPS buffer, pH 7, 20°C. The solid line is an average of three shots and best fit to a double exponential equation I(t) = 0.68 exp −45.5t + 0.32 exp − 5.2t + C. The fast phase is a direct measure of the rate of Pi dissociation from regulated actomyosin-S1-ADP-Pi. Interpretation of the slow phase is complicated by there being more than one possible route of breakdown for the M-ATP pool, including attached hydrolysis. **(C and D)** Double mixing experiments performed with md-ATP and all cardiac proteins, myosin-S1, and native thin filaments. Data taken from Houmeida et al. (2010). **(C)** Phosphate dissociation from "turned-off" (no bound ligands) regulated AM-md-ADP-Pi. First mix, 2 µM cardiac myosin-S1 + 3 µM md-ATP. Delay, 2 s. Second mix, 47 µM native cardiac thin filaments containing 2.0 mM EGTA and 2 mM MgATP. Final concentrations in flow cell: 0.44 µM cardiac S1, 0.67 µM nucleotide, 26 µM cardiac thin filaments (0.55 mM EGTA), 1.1 mM MgATP, 2 mM $MgCl_2$, and 5 mM MOPs, pH 7, 20°C. Ionic strength, 13.5 mM. The averaged solid line is the best fit to a single exponential equation I(t) = I.0 exp −0.37t + C. **(D)** Phosphate dissociation from "turned-on" (bound Ca[II] and bound rigor myosin-S1) regulated AM-md-ADP-Pi. Conditions as in C, except 19 µM cardiac S1 was used in the first mix, final concentration 3.8 µM, and the thin filaments contained 0.3 mM $CaCl_2$ and no MgATP. Ionic strength, 12 mM. The averaged solid line is the best fit to a double exponential equation I(t) = 0.76 exp −25t + 0.24 exp − 1.9t + C. The fast phase is a direct measure of the rate of Pi dissociation from regulated actomyosin-S1-md-ADP-Pi. Interpretation of the slow phase is complicated for the reasons given in B.

myosin-ADP-Pi within the dead-time of the second mix, and the fluorescence trace consists of two components. The faster of the two phases stems from dissociation of Pi from AM-ADP-Pi, whereas the slower emanates from the AM-ATP population in which the rate is limited by the rate of hydrolysis of the ATP bound to AM (see Scheme 1). At 20°C, the maximum rates of the two phases, extrapolated from their concentration dependences, are 75 and 3 s^{-1} (White et al., 1997; Table 1). This study also provided clear evidence for an ordered release of products, Pi followed by ADP.

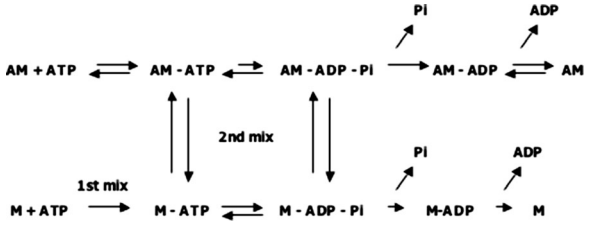

(Scheme 1)

Regulation of Pi release by thin filaments

In a follow-up to White et al. (1997), regulatory proteins (whole troponin and tropomyosin) were prepared from rabbit skeletal muscle consisting mostly of fast contracting fibers. Because there is variation between different preparations of isolated troponin, reconstituted thin filaments were first assessed by steady-state ATPase assay. Those batches of troponin that produced thin filaments that gave at least 15-fold Ca(II) sensitivity (mole ratio of S1: actin = 1:70 to 1:120; low ionic strength) of the rate were selected for use. The rate of Pi release (i.e., AM-ADP-Pi → AM-ADP + Pi) was demonstrated to be acutely sensitive to the association of Ca(II) and rigor myosin with the thin filament (Heeley et al., 2002) but not in a way predicted by the Three-State or classical Steric Blocking models. When the thin filaments are turned off (i.e., apo, no bound ligands; i.e. , EGTA, and zero rigor), the fluorescence increase is slow and monophasic (Fig. 2 A) and the maximum rate, k obs, at saturation is 0.64 s^{-1} (Table 1). In all other instances, biphasic kinetics (e.g., Fig. 2 B) are observed with the faster component being attributed to the dissociation of Pi from regulated actomyosin-S1-ADP-Pi. At pCa 4 (zero rigor), k obs is 16 s^{-1}, a 25-fold increase (Table 1). Thus,

Table 1. **Summary of product release kinetic data**

	Apo	Ca(II)	Rigor	Ca(II) + rigor	Actin
Skeletal					
k_{fast} (Pi)	0.64 s^{-1}	16 s^{-1}	30 s^{-1}	77 s^{-1}	75 s^{-1}
Keq $_{TF, fast}$	26 μM	17 μM	12 μM	18 μM	
k_{fast} md-ADP-Pi	0.68 s^{-1}	18 s^{-1}	30 s^{-1}	96 s^{-1}	125 s^{-1}
Keq $_{TF, fast}$	53 μM	26 μM	13 μM	18 μM	68 μM
Cardiac					
k_{fast} (md-ADP-Pi)	0.49 s^{-1}	27 s^{-1}	24 s^{-1}	36 s^{-1}	38 s^{-1}
Keq $_{TF, fast}$	16 μM	19 μM	11 μM	11 μM	53 μM
k_{fast} (md-ADP)	64 s^{-1}	357 s^{-1}	332 s^{-1}	359 s^{-1}	361 s^{-1}
Keq $_{TF, fast}$	32 μM	12 μM	27 μM	6 μM	49 μM

The columns are for thin filaments (low ionic strength, 20°C, pH 7) with no bound ligands (apo); Ca(II) alone, rigor myosin-S1 alone and Ca(II) plus rigor myosin-S1. Actin, unregulated actin. Skeletal, skeletal thin filaments and skeletal myosin-S1A1. Cardiac, native cardiac thin filaments and cardiac myosin-S1. The data are of the fast component of the fluorescence change, which is due to the conversion of AM-NDP-Pi to AM-NDP + Pi. The slower component is not included. k_{fast} (Pi), the maximum rate for the dissociation of Pi (as obtained with fluorescent PBP) from regulated actomyosin-S1-ADP-Pi; k_{fast} (md-ADP-Pi), the maximum rate for dissociation of md-ADP from regulated actomyosin-S1-md-ADP-Pi; k_{fast} (md-ADP), the maximum rate for dissociation of md-ADP from regulated actomyosin-S1-md-ADP. $K_{eq\ TF,\ fast}$, thin filament (actin subunit) concentration at half-maximal rate.

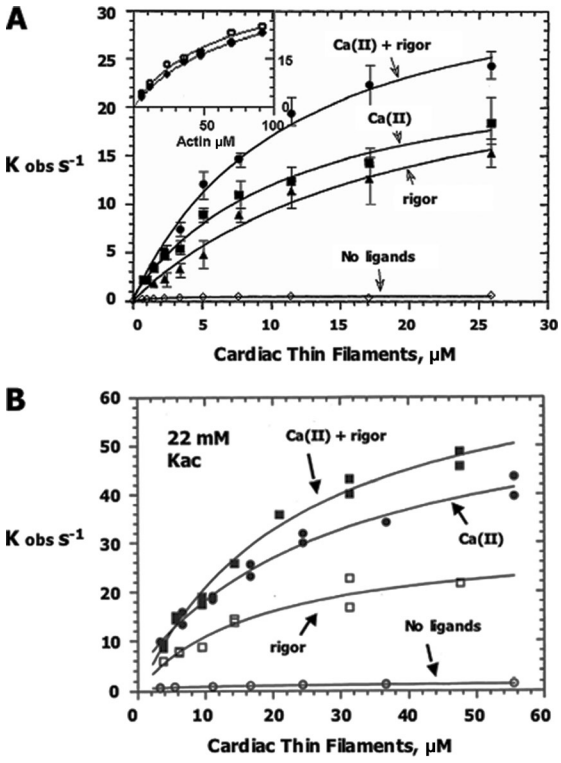

Figure 3. **Dependence of the rates of phosphate dissociation from pre–power stroke myosin at different ionic strengths on the concentration of cardiac thin filaments and ligand binding.** Native thin filaments were isolated from porcine cardiac muscle. Different myosin-S1s were used at the different ionic strengths: Cardiac-S1 (zero added salt; A); Skeletal-S1A1 (22 mM Kac; B). After the second mix, rigor S1 (if present) was at a 1:7 molar ratio to the actin monomer concentration. T, 20°C, pH 7. The solid lines dissecting the data points are best fits to a hyperbolic equation: k obs = k(1 + (K_{TF}/[TF])). Data from Houmeida et al. (2010). **(A)** Phosphate dissociation from regulated AM-ADP-Pi-md-ADP-Pi at low ionic strength (~13 mM, zero added salt) was measured from the fast component as seen in Fig. 2, C and D. Thin filaments with zero rigor S1 contained 2 mM ATP. Note: Only the fast component of the biphasic fluorescence change from md-ADP dissociation is plotted. No bound ligands, k_{fast} = 0.49 s^{-1}, K = 16 μM; Ca(II) alone, k_{fast} = 27 s^{-1}, K = 19 μM; rigor myosin-S1 alone, k_{fast} = 24 s^{-1}, K = 11 μM; Ca(II), and rigor myosin-S1, k_{fast} = 36 s^{-1}, K = 11 μM. Error bars, ≤15% (Fig. 4 legend in Houmeida et al., 2010). Inset, product release from unregulated AM-md-ADP-Pi using md-ATP (open circles), k_{fast} = 38 s^{-1}, K = 53 μM, and fluorescent PBP (closed circles), k_{fast} = 30 s^{-1}, K = 48 μM. **(B)** Phosphate dissociation from regulated AM-ADP-Pi-ADP-Pi in 22 mM potassium acetate. Skeletal myosin-S1A1 and PBP were used. Note: Only the fast component of Pi release is plotted. No bound ligands, k_{fast} = 1.1 s^{-1}, K = 21 μM; Ca(II) alone, k_{fast} = 58.4 s^{-1}, K = 31 μM; rigor myosin-S1 alone, k_{fast} = 30.7 s^{-1}, K = 18 μM; Ca(II); and rigor myosin-S1, k_{fast} = 73 s^{-1}, K = 24 μM.

the effect of Ca(II) is in close agreement with what had been reported earlier under similar conditions: k obs, 1 s^{-1} (apo) and 20–25 s^{-1} (pCa 4; Fig. 3 in Rosenfeld and Taylor, 1987a). The effect of rigor myosin binding was studied at a stoichiometry of one rigor-S1A1 to seven actin subunits. The ratio was selected in light of the dependence of Pi dissociation on the amount of rigor S1A1 bound to the thin filament. Maximal activation was attained at 1 rigor S1 per 14 actin subunits (Fig. 5 of Heeley et al., 2002), suggestive of a regulatory unit that is longer than one molecule of tropomyosin or one that comprises both sides of the thin filament. On the basis of this observation, a ratio of 1:7 was assumed to be sufficient to attain saturation. Under these conditions, the maximum rates of Pi dissociation were 30 s^{-1} (EGTA plus rigor myosin-S1) and 77 s^{-1} (Ca[II] plus rigor myosin-S1), the latter being the same within experimental error as the rate obtained with unregulated actin (Table 1). Similar results were obtained when rigor S1 was premixed with thin filaments (in a "T" mixer) 5–10 min before being used for a double-mixing experiment in which there was no rigor S1 arising from the first mix (Heeley et al., 2002). While a redistribution of bound heads cannot be ruled out, the lack of an observed effect of premixing on Pi dissociation kinetics indicates that a redistribution either did not occur or was of little consequence. Therefore, from the PBP-based observations, which are a direct measure of the active site departure of Pi, it became evident that both ligands are required for full activation (a fold increase of >100), whereas rigor-bound heads alone are insufficient. At the same time, Ca(II) and rigor myosin had only a small effect, approximately twofold, on the affinity of thin filaments for myosin-ADP-Pi (Table 1).

Similar findings were reported in a parallel study (Heeley et al., 2006) conducted with the deoxyribose modified analogue mant-ATP or 2′ deoxymethanthranolyl (md)–ATP (Hiratsuka, 1983). The strategy, which hinged on a sequential departure of products from the active site of myosin, allowed for the inclusion of mM MgATP in the reconstituted thin filaments (skeletal) to prevent unwanted rigor activation, something that had been a concern in the fluorescent PBP experiments. Using

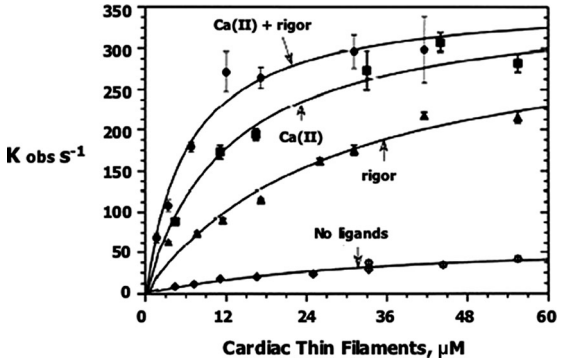

Figure 4. **Dependence of the rates of product dissociation from post–power stroke myosin on the concentration of cardiac thin filaments and ligand binding.** md-ADP release from regulated AM-md-ADP (post–power stroke configuration) at low ionic strength (~13 mM) and at 20°C. Conditions same as in Fig. 3 A except md-ATP was replaced by md-ADP in the first mix. Second mix, thin filaments (of varying concentration) plus 2 mM MgATP. The observed time course of the fluorescence change at each individual concentration conformed to a single exponential process (Houmeida et al., 2010). The rate constants for md-ADP dissociation are as follows: no bound ligands, k = 64 s^{-1}, K = 32 μM; Ca(II) alone, k = 357 s^{-1}, K = 12 μM; rigor myosin-S1 alone, k = 332 s^{-1}, K = 27 μM; Ca(II) and rigor myosin-S1, k = 359 s^{-1}, K = 6 μM. Note: The rates of dissociation of md-ADP from cardiac actomyosin-S1-md-ADP are about six times faster than those for native ADP at 15°C (Siemankowski and White, 1984).

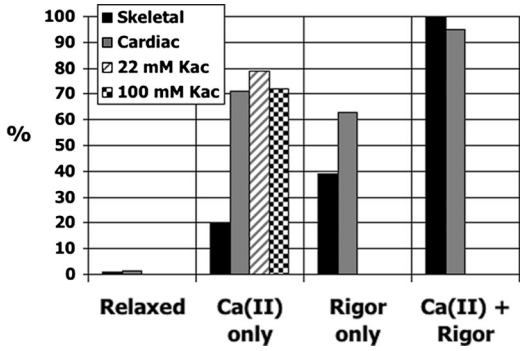

Figure 5. **Comparison of the activation of different types of thin filaments by Ca(II) and rigor myosin-S1.** The maximum rate of phosphate dissociation from regulated actomyosin-NDP-Pi is expressed as a percentage of the maximum unregulated rate. The ligand condition is indicated. All measurements were with md-ATP except those represented by black bars. Black bars, measurements using fluorescent PBP with all skeletal proteins at low ionic strength (zero added salt; Heeley et al., 2002); gray bars, all cardiac proteins at low ionic strength (zero added salt; Houmeida et al., 2010). Striped and checkered bars, native cardiac thin filaments (bound Ca[II] only) in, respectively, 22 and 100 mM potassium acetate and using skeletal myosin-S1A1 (Risi et al., 2017). Error, ≤15%.

md-ATP, the fold-activations of the product release kinetics for the various ligand combinations are in line with what is observed with PBP (Table 1).

These observations (Heeley et al., 2006) added support to the view that Pi release (AM-ADP-Pi → AM-ADP + Pi) is the primary regulated step of the mechanism.

Cardiac versus skeletal thin filaments

The isomorphisms that exist between the two sets of regulatory proteins, those in heart and fast skeletal muscle, chiefly reside in the troponin complex, notably the T subunit (reviewed in Wei and Jin, 2016). Cardiac myosin-S1 (which has slower kinetics and weaker affinity for actin than skeletal-S1A1; Siemankowski et al., 1985) and native thin filaments were isolated from porcine ventricle. Transient kinetic analysis of the cardiac system was performed using md-ATP. As stated earlier, the fluorescence nucleotide allowed mM MgATP to be used to ensure that no rigor myosin was bound to the thin filaments. Selected time-course recordings are presented in Fig. 2, C and D. Compared with the skeletal muscle counterpart, there are similarities and differences. The rate constants for cardiac thin filament-induced acceleration of dissociation of md-ADP from regulated-AM-md-ADP-Pi are as follows: 0.49 s^{-1} (no bound ligands), 24 s^{-1} (rigor myosin-S1 only), 27 s^{-1} (Ca[II] only), and 36 s^{-1} (Ca[II] plus rigor myosin-S1; see Fig. 3 A and Table 1). The fold difference between fully activated and inhibited cardiac thin filaments is ~80 (Houmeida et al., 2010). Thus, it is apparent that each type of thin filament requires both Ca(II) and rigor S1 binding for full activation, but the cardiac system is more responsive to an individual ligand. For example, Ca(II) alone yields >70% of the maximum observed rate when the thin filament is fully activated. The heightened ligand sensitivity may be related to the fact that the cardiac thin filaments were not reconstituted. That is, they were not assembled in vitro from individual components. More interestingly, it may be a consequence of the comparatively longer length of the predominant cardiac troponin-T isoform (Pearlstone et al., 1986).

The pronounced activation by Ca(II) is also observed at higher ionic strengths, 22 and 100 mM potassium acetate (Kac). For these experiments, skeletal myosin-S1A1 was preferred to cardiac-S1 owing to it having a higher activity. In 22 mM acetate (20°C, pH 7), the concentration dependences of Pi release are well fit by hyperbolic functions: 1.1 s^{-1} (no bound ligands), 58.4 s^{-1} (Ca[II] alone), and 73 s^{-1} (Ca[II] plus rigor myosin-S1; Fig. 3 B). At the higher concentration of salt (100 mM Kac), the rate of product dissociation is linearly dependent upon the thin filament concentration. The second order rate constants are as follows: 2 × 10^3 M^{-1} s^{-1} (no bound ligand), 1.3 × 10^5 M^{-1} s^{-1} (Ca[II] alone), and 1.8 × 10^5 M^{-1} s^{-1} (Ca[II] plus rigor myosin-S1; Figs. S6 and S7 and Table ST1 in Risi et al., 2017). Thus, the percent activation observed with a mixture of isotypes is similar to that obtained at low ionic strength with protein components derived solely from heart (Fig. 3 A). Specifically, the activation by Ca(II) alone in 22 and 100 mM acetate is >70% of the maximum. The agreement is illustrated by the bar graph in Fig. 5.

Thin filament regulation of post–power stroke myosin

A key question is whether post–power stroke myosin (having an "open" switch II conformation) is equivalent in terms of its regulation to that of myosin containing ADP-Pi in the active site (pre–power stroke, "closed" switch II conformation). This was investigated via the same procedure that has been described except that a fluorescent analogue of ADP (instead of ATP) was employed in the first mix. With etheno-ADP and all skeletal muscle proteins, the rate is increased 15-fold by Ca(II) binding

(Rosenfeld and Taylor, 1987b). With deoxyribose mant-ADP (md-ADP), which has faster dissociation kinetics than native ADP (Siemankowski and White, 1984), and all cardiac proteins, the change is smaller, some sixfold (Fig. 4; Houmeida et al., 2010). Further, when used individually or together, Ca(II) and rigor myosin-S1 all brought about a similar increase in the release rate of the nucleoside diphosphate (from regulated AM-md-ADP). The maximum rates at 20°C are 64 s^{-1} (no bound ligands), 357 s^{-1} (Ca[II] alone), 332 s^{-1} (rigor myosin-S1 alone), and 359 s^{-1} (Ca[II] plus rigor myosin-S1). It is apparent, therefore, that regulation is significantly diminished in scale compared to when myosin-S1 has both products, ADP and Pi, in the active site (Fig. 3 A).

Conclusions

Phosphate dissociation (from regulated actomyosin-S1-ADP-Pi) is generally accepted to be the stage in the contraction of striated muscle that produces force (reviewed in Houdusse and Sweeney, 2016). The authors have investigated the regulation of this step in transient kinetic experiments designed to mimic a working actomyosin cycle. This approach differs from that of other work, such as steady-state kinetics and myosin binding to the thin filament, in that it monitors the rate of decay of the pre–power stroke complex (regulated actomyosin-S1-ADP-Pi). Comparison of four defined conditions, (1) no bound ligands, (2) maximal activation by Ca(II), (3) maximal activation by rigor myosin, and (4) maximal activation by Ca(II) and rigor myosin together, reveals a strong dependence of the rate of Pi release on the liganded state of the thin filament. In other words, this part of the AM cycle is a regulatory focal point. Our observations, which have been overlooked, are at odds with the Three-State model (McKillop and Geeves, 1993) that was formulated to account for the association of strong binding myosin intermediates with the thin filament. Points of disagreement are as follows.

First, the maximum acceleration of Pi release of 80–140-fold (depending on the source of the thin filaments) requires the association of both Ca(II) and rigor myosin-S1 with the thin filament. That is, either ligand by itself is insufficient to fully activate the thin filament. The Three-State model predicts maximal activation by rigor binding alone.

Second, thin filaments containing only bound Ca(II) accelerate Pi release by 25–50-fold relative to inactivated thin filaments (EGTA, zero rigor; Table 1). The model predicts a smaller effect of Ca(II). The extent of cardiac thin filament activation by Ca(II) alone (>70% of maximum) is observed over a range of ionic strengths (Fig. 3 B and Fig. 5). From this it is evident that Ca(II) is the main thin filament activator in heart and that any rigor-bound heads that arise during the course of a contraction will have only a relatively small additional effect. Thus, there is quantitative disagreement between the transient kinetic results and the degree to which the three states of skeletal and cardiac thin filaments are populated at different concentrations of Ca(II) (Maytum et al., 2003).

What is the reason for the lack of agreement? A realistic kinetic model of regulation of the actomyosin ATP hydrolysis cycle that occurs in muscle must account for the regulation of ATP hydrolysis and the power stroke. Experimental scenarios where ATP hydrolysis is not taking place are unlikely to provide satisfactory models for regulation and appear to be monitoring other interesting aspects of the system. We contend that a major source of disagreement is the nonequivalence of pre– or post–power stroke myosin with respect to activation of the thin filament. Thus, the level of regulation depends not only on the thin filament state but the conformation of myosin as well.

Finally, the pattern of regulation that we have characterized has been fit to an allosteric model comprising two states, inactive and active, that differ in their ability to activate Pi release (Scheme 2). In the case of apo thin filaments, the equilibrium strongly favors the inactive state. The association of Ca(II) and rigor heads to the thin filament shifts the equilibrium toward the active conformer to varying degrees depending on protein isotype. But in both instances (skeletal and cardiac), maximal activation requires that both ligands are associated with the thin filament.

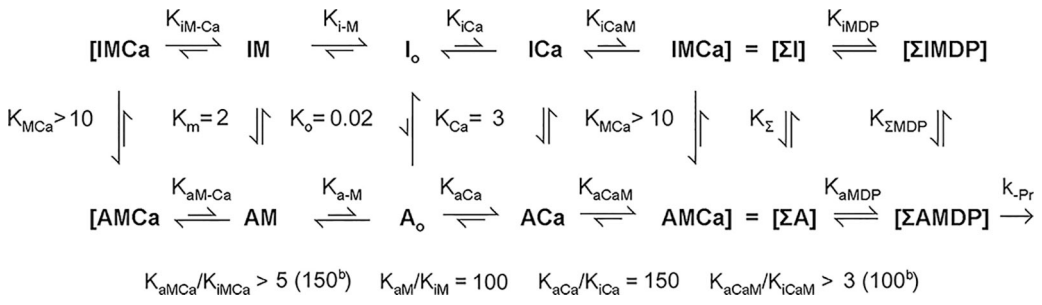

Scheme 2. **Two-state model taken from Houmeida et al. (2010) for cardiac myosin-S1 and cardiac native thin filaments.** A, active thin filament conformation (accelerates product dissociation from M-ADP-Pi); I, inactive thin filament conformation (does not accelerate product release from M-ADP-Pi); subscripts to equilibrium constants i = inactive thin filament conformation and a = active thin filament conformation; if neither i nor a is indicated, the equilibrium constant is the apparent equilibrium constant [A(Ca,M)]/[I(Ca,M)], with the indicated ligands bound to the thin filament (e.g., K_{Ca} is the equilibrium between A and I with calcium bound to the thin filament, and K_{iCa} is the association constant for calcium binding to the inactive filaments (I); M, cardiac S1; Ca, calcium; the second subscript is the associating/dissociating ligand. ∑A and ∑I are the sum of the active and inactive thin filament regulatory units. The values for the equilibrium constants or ratios of equilibrium constants assuming that the affinity is only a function of the thin filament conformation and not of the bound ligands (i.e., $K_{iCa} = K_{iMCa}$, $K_{aCa} = K_{aMCa}$, $K_{iM} = K_{iCaM}$, and $K_{aM} = K_{aCaM}$) are shown in parentheses.

Acknowledgments

This work was supported by Canadian Institutes of Health Research and Natural Sciences and Engineering Research Council of Canada grants to D.H. Heeley; National Institutes of Health grants HL41776 and EB00209 to H.D. White; and National Institutes of Health grants NIH GM1992 and NHLBI HL 20592 and Muscular Dystrophy Association of America grants to E.W. Taylor.

The authors declare no competing financial interests.

Author contributions: The authors contributed equally to the experimentation. The article was written by D.H. Heeley after extensive discussions with H.D. White and E.W. Taylor.

Henk L. Granzier served as editor.

Submitted: 31 July 2018
Revised: 23 October 2018
Accepted: 7 February 2019

References

Bagshaw, C.R., and D.R. Trentham. 1973. The reversibility of adenosine triphosphate cleavage by myosin. *Biochem. J.* 133:323–328. https://doi.org/10.1042/bj1330323

Brune, M., J.L. Hunter, J.E. Corrie, and M.R. Webb. 1994. Direct, real-time measurement of rapid inorganic phosphate release using a novel fluorescent probe and its application to actomyosin subfragment 1 ATPase. *Biochemistry.* 33:8262–8271. https://doi.org/10.1021/bi00193a013

Chalovich, J.M., and E. Eisenberg. 1982. Inhibition of actomyosin ATPase activity by troponin-tropomyosin without blocking the binding of myosin to actin. *J. Biol. Chem.* 257:2432–2437.

Chalovich, J.M., P.B. Chock, and E. Eisenberg. 1981. Mechanism of action of troponin. tropomyosin. Inhibition of actomyosin ATPase activity without inhibition of myosin binding to actin. *J. Biol. Chem.* 256:575–578.

Finlayson, B., and E.W. Taylor. 1969. Hydrolysis of nucleoside triphosphates by myosin during the transient state. *Biochemistry.* 8:802–810. https://doi.org/10.1021/bi00831a007

Haselgrove, J.C. 1972. X-ray evidence for a conformational change in the actin containing filaments of vertebrate striated muscle. *Cold Spring Harb. Symp. Quant. Biol.* 37:341–352. https://doi.org/10.1101/SQB.1973.037.01.044

Heeley, D.H., B. Belknap, and H.D. White. 2002. Mechanism of regulation of phosphate dissociation from actomyosin-ADP-Pi by thin filament proteins. *Proc. Natl. Acad. Sci. USA.* 99:16731–16736. https://doi.org/10.1073/pnas.252236399

Heeley, D.H., B. Belknap, and H.D. White. 2006. Maximal activation of skeletal muscle thin filaments requires both rigor myosin S1 and calcium. *J. Biol. Chem.* 281:668–676. https://doi.org/10.1074/jbc.M505549200

Hill, T.L., E. Eisenberg, and L. Greene. 1980. Theoretical model for the cooperative equilibrium binding of myosin subfragment 1 to the actin-troponin-tropomyosin complex. *Proc. Natl. Acad. Sci. USA.* 77:3186–3190. https://doi.org/10.1073/pnas.77.6.3186

Hill, T.L., E. Eisenberg, and L.E. Greene. 1983. Alternate model for the cooperative equilibrium binding of myosin subfragment-1-nucleotide complex to actin-troponin-tropomyosin. *Proc. Natl. Acad. Sci. USA.* 80:60–64. https://doi.org/10.1073/pnas.80.1.60

Hiratsuka, T. 1983. New ribose-modified fluorescent analogs of adenine and guanine nucleotides available as substrates for various enzymes. *Biochim. Biophys. Acta.* 742:496–508. https://doi.org/10.1016/0167-4838(83)90267-4

Houdusse, A., and H.L. Sweeney. 2016. How myosin generates force on acting filaments. *Trends Biochem. Sci.* 41:989–997. https://doi.org/10.1016/j.tibs.2016.09.006

Houmeida, A., D.H. Heeley, B. Belknap, and H.D. White. 2010. Mechanism of regulation of native cardiac muscle thin filaments by rigor cardiac myosin-S1 and calcium. *J. Biol. Chem.* 285:32760–32769. https://doi.org/10.1074/jbc.M109.098228

Huxley, H.E. 1972. Structural Changes in the actin and myosin containing filaments during contraction. *Cold Spring Harb. Symp. Quant. Biol.* 37:361–376. https://doi.org/10.1101/SQB.1973.037.01.046

Lehman, W. 2017. Switching muscles on and off in steps: The McKillop-Geeves Three-State model of muscle regulation. *Biophys. J.* 112:2459–2466. https://doi.org/10.1016/j.bpj.2017.04.053

Luecke, H., and F.A. Quiocho. 1990. High specificity of a phosphate transport protein determined by hydrogen bonds. *Nature.* 347:402–406. https://doi.org/10.1038/347402a0

Lymn, R.W., and E.W. Taylor. 1971. Mechanism of adenosine triphosphate hydrolysis by actomyosin. *Biochemistry.* 10:4617–4624. https://doi.org/10.1021/bi00801a004

Maytum, R., B. Westerdorf, K. Jaquet, and M.A. Geeves. 2003. Differential regulation of the actomyosin interaction by skeletal and cardiac troponin isoforms. *J. Biol. Chem.* 278:6696–6701. https://doi.org/10.1074/jbc.M210690200

McKillop, D.F.A., and M.A. Geeves. 1993. Regulation of the interaction between actin and myosin subfragment 1: evidence for three states of the thin filament. *Biophys. J.* 65:693–701. https://doi.org/10.1016/S0006-3495(93)81110-X

Parry, D.A., and J.M. Squire. 1973. Structural role of tropomyosin in muscle regulation: analysis of the x-ray diffraction patterns from relaxed and contracting muscles. *J. Mol. Biol.* 75:33–55. https://doi.org/10.1016/0022-2836(73)90527-5

Pearlstone, J.R., M.R. Carpenter, and L.B. Smillie. 1986. Amino acid sequence of rabbit cardiac troponin T. *J. Biol. Chem.* 261:16795–16810.

Risi, C., J. Eisner, B. Belknap, D.H. Heeley, H.D. White, G.F. Schröder, and V.E. Galkin. 2017. Ca^{2+}-induced movement of tropomyosin on native cardiac thin filaments revealed by cryoelectron microscopy. *Proc. Natl. Acad. Sci. USA.* 114:6782–6787.

Rosenfeld, S.S., and E.W. Taylor. 1987a. The mechanism of regulation of actomyosin subfragment 1 ATPase. *J. Biol. Chem.* 262:9984–9993.

Rosenfeld, S.S., and E.W. Taylor. 1987b. The dissociation of 1-N6-ethenoadenosine diphosphate from regulated actomyosin subfragment 1. *J. Biol. Chem.* 262:9994–9999.

Secrist, J.A. III, J.R. Barrio, N.J. Leonard, and G. Weber. 1972. Fluorescent modification of adenosine-containing coenzymes. Biological activities and spectroscopic properties. *Biochemistry.* 11:3499–3506. https://doi.org/10.1021/bi00769a001

Siemankowski, R.F., and H.D. White. 1984. Kinetics of the interaction between actin, ADP, and cardiac myosin-S1. *J. Biol. Chem.* 259:5045–5053.

Siemankowski, R.F., M.O. Wiseman, and H.D. White. 1985. ADP dissociation from actomyosin subfragment 1 is sufficiently slow to limit the unloaded shortening velocity in vertebrate muscle. *Proc. Natl. Acad. Sci. USA.* 82:658–662. https://doi.org/10.1073/pnas.82.3.658

Taylor, E.W., R.W. Lymn, and G. Moll. 1970. Myosin-product complex and its effect on the steady-state rate of nucleoside triphosphate hydrolysis. *Biochemistry.* 9:2984–2991. https://doi.org/10.1021/bi00817a008

Wei, B., and J.-P. Jin. 2016. TNNT1, TNNT2, and TNNT3: Isoform genes, regulation, and structure-function relationships. *Gene.* 582:1–13. https://doi.org/10.1016/j.gene.2016.01.006

White, H.D., B. Belknap, and M.R. Webb. 1997. Kinetics of nucleoside triphosphate cleavage and phosphate release steps by associated rabbit skeletal actomyosin, measured using a novel fluorescent probe for phosphate. *Biochemistry.* 36:11828–11836. https://doi.org/10.1021/bi970540h